Gases in Capillaries in the Transition Region between Knudsen and Molecular Diffusion," *Ind. Eng. Chem. Fundamentals*, 12, 214 (1973).
Rothfeld, L. B., "Gaseous Counterdiffusion in Catalyst Pallets," *AIChE J.*, 9, No. 1, 19-24 (1963).
Satterfield, C. N., and P. J. Cadle, "Diffusion and Flow in Commercial Catalysts at Pressure Levels about Atmospheric," *J. Ind. Eng. Chem. Fundamentals*, 7, 202 (1968).
Scott, D. S., and F. A. L. Dullien, "Diffusion of Ideal Gases in Capillaries and Porous Solids," *AIChE J.*, 8, No. 1, 113-117 (1962).
Wheeler, A., *Catalysis*, Vol. 2, Reinhold, New York (1955).
Wilke, C. R., "A Viscosity Equation for Gas Mixtures," *J. Chem. Phys.*, V. 18, No. 4, pp. 517-519 (1950).
Youngquist, G. R., "Diffusion and Flow of Gases in Porous Solids," in *Flow Through Porous Media*, American Chemical Society Publications (1970).

Manuscript received January 19, 1977; revision received August 18, and accepted August 24, 1977.

Collocation Solution of Creeping Newtonian Flow Through Periodically Constricted Tubes with Piecewise Continuous Wall Profile

MARIANO A. NEIRA
and
A. C. PAYATAKES

Chemical Engineering Department
University of Houston
Houston, Texas 77004

A collocation solution of creeping Newtonian flow through periodically constricted tubes is obtained. The profile of the wall of the type of tube considered is piecewise continuous, composed of symmetric parabolic segments. A transformation of the domain of interest into a rectangular one is obtained, which allows satisfaction of all boundary conditions. The collocation solution gives the stream function in terms of the new independent variables and can easily be converted to the original cylindrical coordinates. Axial and radial velocity components are obtained in analytical form, and the pressure drop is calculated from a volume integration of the viscous dissipation function as well as from line integration of the Navier-Stokes equation. The results are compared with the finite-difference solution by Payatakes et al. (1973*b*) and are found in good agreement. Differences between the two solutions are attributed mainly to discretization error in the finite-difference solution. The analytical expressions obtained from the collocation solution can be used together with porous media models of the constricted unit cell type for the modeling of processes taking place in granular porous media.

SCOPE

The problem of laminar flow through periodically constricted tubes usually arises in connection with porous media modeling. Petersen (1958) used this concept to derive an expression for the effective diffusion coefficient in porous pellets. Houpeurt (1959), independently, considered periodically constricted tubes as building elements in his analysis of flow through porous media. These authors, however, did not propose a method for the determination of the geometry of the periodically constricted tubes from experimental measurements, nor did they solve the associated flow problem.

Payatakes, Tien, and Turian (1973*a*) developed a model for granular porous media which employs unit cells that resemble segments of constricted tubes and the geometry and size distribution of which are determined from simple experimental measurements. They postulated that the flow through a given unit cell is identical to that through a segment of the corresponding periodically constricted tube. The latter problem was solved in Payatakes, Tien, and Turian (1973*b*) using a finite-difference method of the stream function-vorticity type. That method can be applied to periodically constricted tubes with different types of wall geometries, even with discontinuities (see also Payatakes, Tien, and Turian, 1973*c*), and it retains the nonlinear terms of the equation of motion. The porous media model of Payatakes et al. (1973*a, b*) was used as basis for the modeling of liquid filtration in deep granular beds with good results (Payatakes, Tien, and Turian, 1974*a, b*; Payatakes, Brown, and Tien, 1977; Rajagopalan and Tien, 1976).

Payatakes and Neira (1977) developed a generalized version of the Payatakes et al. (1973*a*) model by including the random orientation of the unit cells and superimposing a random network structure which accounts for the pore interconnectivity.

Slattery (1974) and Oh and Slattery (1976) used periodically constricted tubes in the analysis of the forces acting on oil ganglia during tertiary oil recovery by flooding in

0001-1541/78/9195-0043/$01.35

an effort to analyze ganglia mobilization and motion. Stegermeier (1976) also used the concept of constricted tubes in considering the factors affecting oil ganglia entrapment and mobilization.

Sheffield and Metzner (1976) made an evaluation of pressure drop vs. flow rate data for nonlinear fluid flow through porous media and concluded that in such cases the converging-diverging character of the flow channels is a dominant factor which may not be neglected.

The finite-difference solution obtained by Payatakes et al. (1973*b*) has the advantages of being applicable to Newtonian flows through periodically constricted tubes of arbitrary geometry and of including the nonlinear inertial terms of the Navier-Stokes equation. On the other hand, it requires large computer memory, and it renders the solution in matrix form. Values of the stream function and the velocity components at off-node points must be determined by two-dimensional interpolation. It is evident, then, that solutions in analytical form are highly desirable.

Perturbation solutions for the flow through sinusoidal tubes, including nonlinear terms, were obtained independently by Dodson, Townsend, and Walters (1971) and Chow and Soda (1972). Unfortunately, these solutions apply only to cases of tubes with relatively small wave amplitudes. They also fail in the case of walls with discontinuities.

In a recent publication, Fedkiw and Newman (1977) presented a collocation solution through periodically constricted tubes. Their solution is quite general and applies to wall geometries with small or large wave amplitudes. A collocation solution of the same problem was also obtained by Neira and Payatakes (1978). The main limitation of these solutions seems to be that they do not apply rigorously to cases where the tube wall has discontinuities (cusps, etc.). In the same publication, Fedkiw and Newman (1977) applied the collocation solution of the flow to the study of mass transfer at high Peclet numbers.

The Payatakes, Tien, and Turian (1973*a*) and the Payatakes and Neira (1977) porous media models involve periodically constricted tubes with walls that have discontinuities (cusps). Such geometry is thought to be more realistic for certain applications, as for instance deep-bed filtration modeling, etc.

The present work is concerned with the development of a collocation solution for this latter type of periodically constricted tubes.

CONCLUSIONS AND SIGNIFICANCE

A collocation solution of creeping Newtonian flow through periodically constricted tubes composed of segments which are parabolas of revolution is obtained. To this end, a transformation of the domain of interest (half a segment) into a rectangular one is obtained, which allows satisfaction of all boundary conditions, Equations (15) and (16). The collocation solution expresses the stream function in terms of the transformed independent variables, Equation (18), and can be converted easily to the original cylindrical coordinates. The axial and radial velocity components are also obtained in analytical form, Equations (23) and (24). The pressure drop along a tube segment is calculated both from a volume integration of the viscous dissipation function and from line integration of the equation of motion.

The method is demonstrated with sample calculations. It is shown that in most cases of interest the collocation solution converges for sixteen or more points and that very good approximations are achieved with only nine collocation points. The collocation expansion coefficients for several different tube geometries are given in Table 4.

The pressure drop for $N_{Re} = 1$ (neglecting inertial effects) is calculated for several representative geometries, Table 5, and the results are presented in graph form, Figure 9. The results are compared with the finite-difference solution by Payatakes et al. (1973*b*) and are found in agreement. Differences between the two solutions are attributed mainly to discretization error in the latter.

The advantages of the present solution over that in Payatakes et al. (1973*b*) are that it gives the results in analytical form, it requires substantially less computer memory, and it achieves appreciably greater accuracy with less computational effort. On the other hand, it does not take in account the inertial effects, thus being valid only under creeping flow conditions, and unlike the finite-difference method, it requires some modifications if it is to be applied to a type of tube geometry other than the one considered here. The wall geometry of the periodically constricted tube considered in the present work is similar to that used in the models by Payatakes, Tien, and Turian (1973*a*) and Payatakes and Neira (1977). Thus, the present solution can be used for the study of transfer processes taking place in granular porous media.

STATEMENT OF THE PROBLEM

Let (r^*, θ, z^*) be dimensionless cylindrical coordinates, Figure 1, with r^* and z^* defined by

$$r^* = \frac{r}{h}, \quad z^* = \frac{z}{h} \tag{1}$$

where r and z are the corresponding dimensional coordinates. The origin is placed at the center of a cross section of minimum diameter, Figure 1. The dimensionless radius of the tube wall, r_w^* is given by

$$r_w^*(z^*) = \begin{cases} r_1^* + 4(r_2^* - r_1^*)z^{*2} & \text{for } 0 \leq z^* \leq \tfrac{1}{2} \\ r_1^* + 4(r_2^* - r_1^*)(1 - z^*)^2 & \text{for } \tfrac{1}{2} \leq z^* \leq 1 \end{cases} \tag{2}$$

We have

$$v_o = \frac{q}{\pi(r_1^* h)^2} \tag{3}$$

Let v_z, v_r, p, and P be the dimensional axial velocity component, radial velocity component, thermodynamic pressure and total pressure, respectively; the dimensionless counterparts are defined by

$$v_z^* = \frac{v_z}{v_o}, \quad v_r^* = \frac{v_r}{v_o} \tag{4}$$

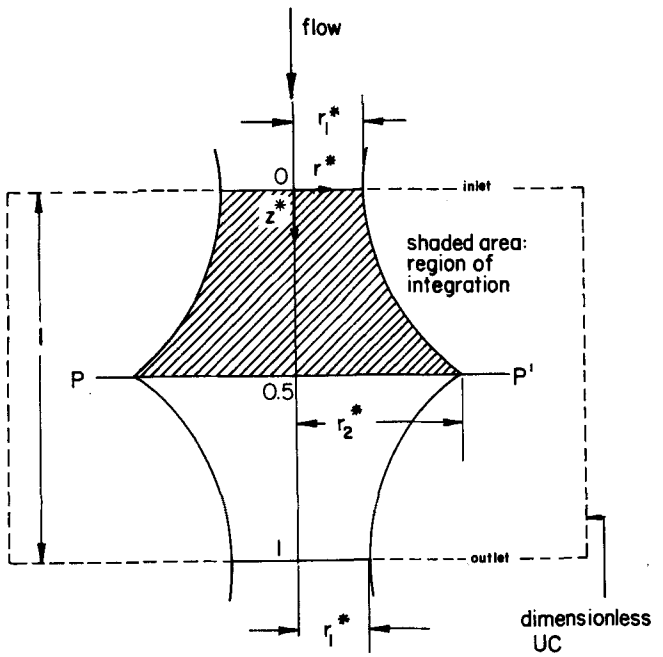

Fig. 1. Dimensionless periodically constricted tube.

$$P^* = \frac{P}{\rho v_o^2} = \frac{p - \rho g z}{\rho v_o^2} \tag{5}$$

The Reynolds number is defined as

$$N_{Re} = \frac{\rho v_o h}{\mu} \tag{6}$$

If we define a dimensionless stream function ψ^* by

$$v_r^* = \frac{1}{r^*}\frac{\partial \psi^*}{\partial z^*}, \quad v_z^* = -\frac{1}{r^*}\frac{\partial \psi^*}{\partial r^*} \tag{7}$$

the equation of motion for steady creeping flow becomes

$$E^{*4}\psi^* = 0 \tag{8}$$

where the operator E^{*2} is defined by

$$E^{*2} \equiv \frac{\partial^2}{\partial r^{*2}} - \frac{1}{r^*}\frac{\partial}{\partial r^*} + \frac{\partial^2}{\partial z^{*2}} \tag{9}$$

Equation (8) is to be integrated with the following boundary conditions:

1. The no-slip condition requires that

$$\psi^* = \frac{\partial \psi^*}{\partial r^*}\left(= \frac{\partial \psi^*}{\partial z^*}\right) = 0 \quad \text{at} \quad r^* = r_w^*(z^*) \tag{10}$$

An integral mass balance over a cross-sectional area of the tube yields

$$\psi^*(0, z^*) = r_1^{*2}/2 = \text{constant} \tag{11}$$

2. The axial symmetry of the flow requires that

$$\left(\frac{1}{r^*}\frac{\partial \psi^*}{\partial z^*} =\right) \frac{\partial}{\partial r^*}\left(\frac{1}{r^*}\frac{\partial \psi^*}{\partial r^*}\right) = 0 \quad \text{at} \quad r^* = 0 \tag{12}$$

3. The periodicity condition of fully developed flow gives

$$\psi^*(r^*, z^*) = \psi^*(r^*, z^* + i) \tag{13}$$

where i is any integer.

4. Finally, the symmetric nature of the creeping flow requires that

$$\psi^*(r^*, z^*) = \psi^*(r^*, -z^*) \tag{14}$$

Owing to the symmetry and periodicity of the solution, the region of integration can be reduced to the region between the planes $z^* = 0$ and $z^* = \frac{1}{2}$. This region corresponds to the shaded area in Figure 1. The problem thus formulated has a unique solution (Ladyzhenskaya, 1975).

COLLOCATION SOLUTION

In order to simplify the boundary conditions, and consequently the selection of a trial function, it is expedient to transform the region of integration into a rectangular one by introducing a new system of dimensionless coordinates (ξ, η). It is highly desirable that the new system of coordinates (ξ, η) has certain symmetry properties which the solution is expected to have. Several attempts were made to find suitable trial functions which satisfied all the boundary conditions after some simple transformation was tentatively adopted, but without success. Thus, for example, use of the transformation $\xi = r^*/r_w^*$ and $\eta = z^*$ made impossible the selection of a suitable trial function, basically because this transformation does not provide the necessary symmetry about the plane $z^* = \frac{1}{2}$. This particular transformation is suitable in the case of periodically constricted tubes with continuous wall profile, such as sinusoidal tubes, namely in those cases in which $\partial r_w^*/\partial z^*$ vanishes at the cross sections of maximum and minimum diameter. If this transformation is used in the case of wall geometries for which $\partial r_w^*/\partial z^* \neq 0$ at $z^* = \frac{1}{2}$, then it can be shown that $v_r^*(r^*, \frac{1}{2})$ from the collocation solution cannot be made to vanish for all r^* values, as it should under creeping flow conditions.

Because of these difficulties, a method of simultaneous selection of coordinate transformation and trial solution was adopted. According to this method, rather general expressions for ξ, η, and $\psi^*(\xi, \eta)$ were selected first; then, by imposing the required conditions of the problem, the free parameters included in those general expressions were determined. This analytical procedure led simultaneously

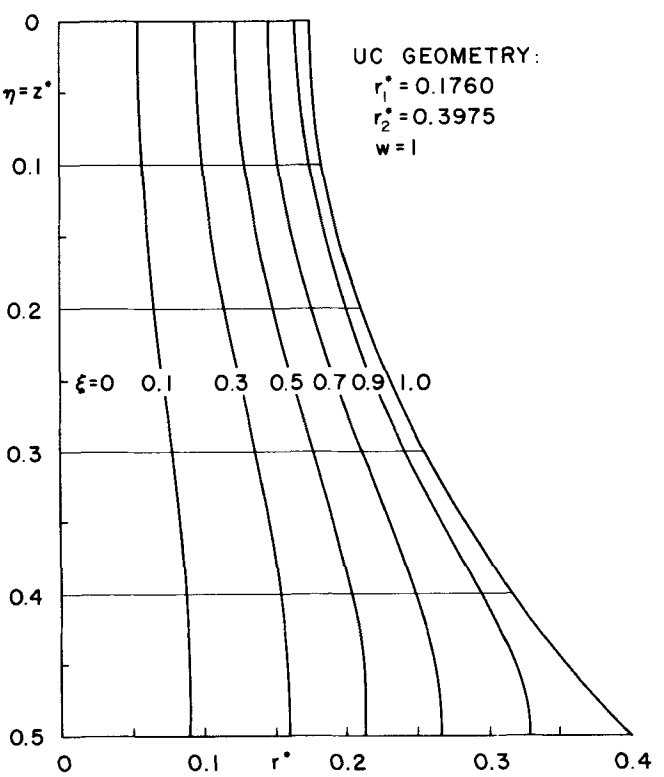

Fig. 2. New coordinate system (ξ, η) for $w = 1$.

to the selection of an appropriate coordinate transformation and of the corresponding trial function (see Neira, 1977, for detailed procedure).

Coordinate Transformation

The new coordinate system (ξ, η) is defined in the following way:

$$\xi(r^*, z^*) = \left(\frac{r^*}{r_w^*}\right)^2 \left[\left[1 - \left(\frac{r^*}{r_w^*}\right)^2\right]\gamma + 1\right] \tag{15}$$

$$\eta(z^*) = z^* \tag{16}$$

where

$$\gamma(z^*) = w - 2(w+1)\left(\frac{r_w^*}{r_2^*}\right) + (w+3)\left(\frac{r_w^*}{r_2^*}\right)^2 \tag{17}$$

and w is an adjustable parameter (for most geometries of interest $w = 1$, see below). The main properties of this transformation are:

1. ξ takes the values 0 and 1 along the center line of the tube and on the wall, respectively; also, ξ is a monotonically increasing function of r^* in this interval.
2. ξ is an even function of z^*, and its first partial derivative with respect to z^* vanishes on the plane $z^* = \frac{1}{2}$; thus the conditions of symmetry and periodicity of the solution can be easily included.

The new coordinate system is illustrated in Figure 2 for the case $w = 1$.

Trial Function

A suitable trial function is

$$\psi_N^*(\xi, \eta) = \psi_o^*(\xi) + \sum_{k=1}^{N} C_k \xi (1-\xi)^{i+1} \cos(j-1)2\pi\eta \tag{18}$$

where

$$\left.\begin{aligned} &\psi_o^*(\xi) = (r_1^{*2}/2)(1-\xi)^2 \\ &k = (j-1)n_r + i \\ &i = 1, \ldots, n_r; \quad j = 1, \ldots, n_z \\ &N = n_r n_z \end{aligned}\right\} \tag{19}$$

and C_k are the as yet unknown expansion coefficients. These coefficients are to be determined by equating the residuals of the differential equation, Equation (8), to zero at N collocation points in the domain of interest of the independent variables. This can be expressed as

$$R_{ij} = R(\xi_i, \eta_j) = 0, \quad i = 1, \ldots, n_r; \quad j = 1, \ldots, n_z \tag{20}$$

where the residuals R_{ij} are formed by substitution of the approximate solution into the differential equation properly transformed in terms of the new system of coordinates. The transformed differential equation is given in Appendix A. The residual equations form a set of N linear equations for the N unknown coefficients C_k.

The collocation points in the η direction will be chosen as the zeroes of the first omitted cosine function of the trial expansion (Mehler quadrature points)

$$\eta_j = (j - 0.5)/(2n_z), \quad j = 1, \ldots, n_z \tag{21}$$

while in the ξ direction, the collocation points will be chosen as the roots of the Jacobi polynomials* $P_{n_r}^{(\alpha,\beta)}(\xi)$, which are defined by the orthogonality property

$$\int_0^1 \xi^\beta (1-\xi)^\alpha P_i^{(\alpha,\beta)}(\xi)\, P_{n_r}^{(\alpha,\beta)}(\xi) d\xi = 0,$$

* Several choices of the parameters α and β will be made.

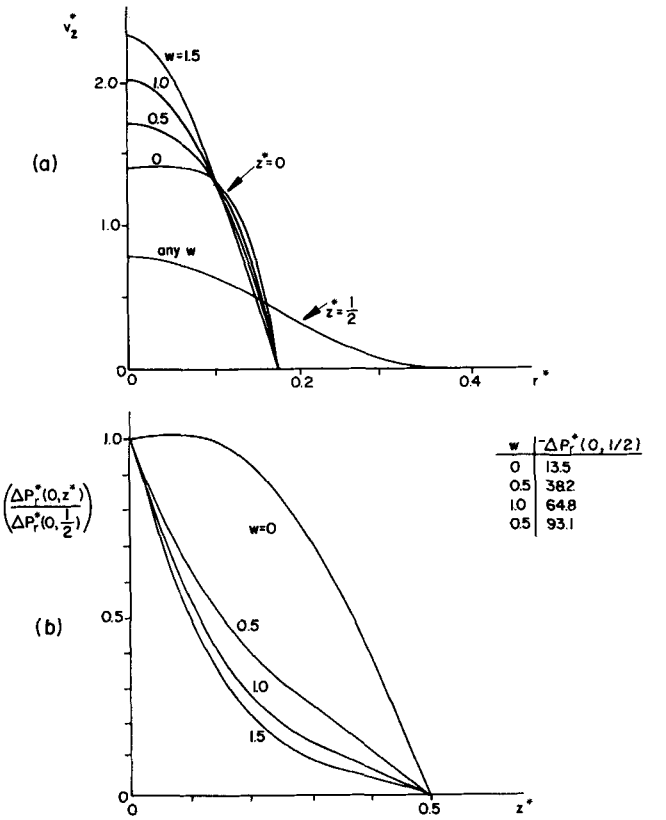

Fig. 3. Approximate solution ψ_o^* for different w values. a) Axial dimensionless velocity profiles. b) Normalized pressure along the axis.

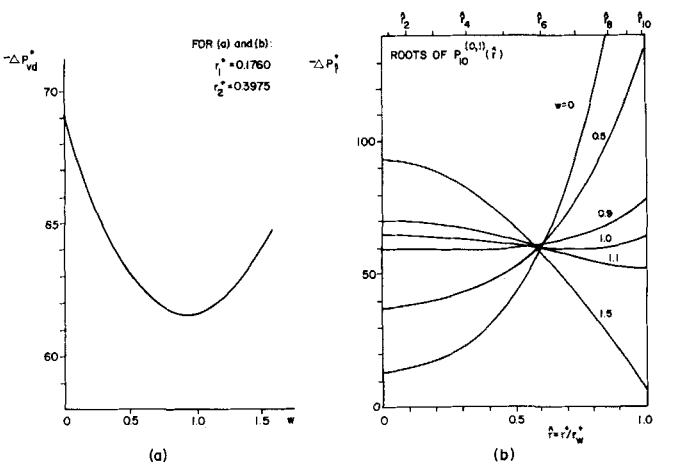

Fig. 4. Approximate solution ψ_o^* for different w values. Dimensionless pressure drop between the planes $z^* = 0$ and $z^* = \frac{1}{2}$.

$$i = 1, \ldots, (n_r - 1) \tag{22}$$

with $\alpha > -1$ and $\beta > -1$. The forms of these polynomials are given in Appendix B.

DETERMINATION OF AXIAL AND RADIAL VELOCITY COMPONENTS

The axial and radial components of the velocity can be obtained in analytical form from the approximate solution ψ_N^* using the following expressions:

$$v_r^* = \frac{1}{r^*}\left[\left(\frac{\partial\xi}{\partial z^*}\right)_{r^*}\left(\frac{\partial\psi^*}{\partial\xi}\right)_\eta + \left(\frac{\partial\psi^*}{\partial\eta}\right)_\xi\right] \tag{23}$$

$$v_z^* = -\frac{1}{r^*}\left(\frac{\partial\xi}{\partial r^*}\right)_{z^*}\left(\frac{\partial\psi^*}{\partial\xi}\right)_\eta \tag{24}$$

TABLE 1. TEST OF CONVERGENCE OF THE COLLOCATION METHOD FOR THE GEOMETRY $r_1^* = 0.1760$ AND $r_2^* = 0.3975$

	$n_r = n_z$					
	0	2	3	4	5	6
$v_z^*(0,0)$	2.026	1.982	1.898	1.916	1.915	1.914
$v_z^*(0,1/2)$	0.784	0.812	0.759	0.752	0.752	0.752
$-2\Delta P^*_{vd}$ $(N_{Re} = 1)$	123.136	122.874	122.448	122.444	122.442	122.442

TABLE 2. COLLOCATION SOLUTION WITH $n_r = n_z = 4$ FOR DIFFERENT SELECTIONS OF COLLOCATION POINTS† ON ξ AND VARIOUS w VALUES. DIMENSIONLESS AXIAL VELOCITY AND PRESSURE DROP FOR $r_1^* = 0.1760$ AND $r_2^* = 0.3975$

		$v_z^*(0, z^*)$			$-\Delta P^* \hat{r}_i$ for $\hat{r}_i$ = roots of $P_{10}^{(0,1)}(\hat{r})$				
w	(α, β)	$z = 0$	$z^* = \frac{1}{2}$	$-\Delta P^*_{vd}$	$\hat{r}_2$	$\hat{r}_4$	$\hat{r}_6$	$\hat{r}_9$	$\hat{r}_{10}$
1.0	(1, 0)	1.916	0.756	61.229	61.74	61.34	61.11	60.17	61.00
1.0	(2, 0)	1.916	0.754	61.227	61.64	61.37	61.00	60.32	62.06
1.0	(3, 0)	1.916	0.752	61.224	61.61	61.38	60.90	60.58	62.70
1.0	(3, 1)	1.916	0.752	61.225	61.52	61.44	60.91	60.48	62.36
1.0	(2, 1)	1.916	0.751	61.227	61.34	61.53	60.94	60.32	61.67
1.0	(1, 1)	1.916	0.754	61.228	60.57	61.97	60.76	60.39	60.75
0.5	(3, 0)	1.915	0.749	61.223	61.54	61.37	60.95	60.44	64.63
1.0	(3, 0)	1.916	0.752	61.224	61.61	61.38	60.90	60.58	62.70
1.5	(3, 0)	1.917	0.756	61.226	61.69	61.41	60.82	60.71	60.91

† ξ_i = roots of $P_i^{(\alpha,\beta)}(\xi)$.

DETERMINATION OF PRESSURE DROP

The pressure drop along one tube segment is calculated numerically from the approximate solution ψ_N^* in two ways:

1. By volume integration of the viscous dissipation function over half a tube segment. The pressure drop calculated with this method will be denoted by ΔP^*_{vd}. We have (see Bird, Stewart, and Lightfoot, 1960):

$$-\Delta P^*_{vd} = \frac{2}{N_{Re}\pi {r_1^*}^2} \int_{V^*} \Phi_v^* dV^* \tag{25}$$

where

$$\Phi_v^* = 2\left[\left(\frac{\partial v_r^*}{\partial r^*}\right)^2 + \left(\frac{v_r^*}{r^*}\right)^2 + \left(\frac{\partial v_z^*}{\partial z^*}\right)^2\right] + \left[\frac{\partial v_r^*}{\partial z^*} + \frac{\partial v_z^*}{\partial r^*}\right]^2 \tag{26}$$

Φ_v^* can be easily expressed in analytical form in terms of ψ_N^* and its derivatives. (For details, see Neira, 1977.) The volume integration of Equation (25) is performed numerically using a double quadrature formula:

$$-\Delta P^*_{vd} \simeq \frac{1}{2N_{Re}{r_1^*}^2} \sum_{i=1}^{m} \sum_{j=1}^{n} w_i w_j ({r_w^*}^2 \Phi_v^*)_{r_{ij}^*, z_j^*} \tag{27}$$

Here $\{z_j^*\}$ correspond to the roots of the Jacobi polynomial $P_n^{(0,0)}(2z^*)$, $\{r_{ij}^*\}$ correspond to the roots of the Jacobi polynomial $P_m^{(0,1)}[r^*/r_w^*(z_j^*)]$ for $j = 1, \ldots, n$, and w_i and w_j are the corresponding normalized Gaussian weights (Villadsen, 1970).

2. By line integration of the equation

$$dP^* = \frac{\partial P^*}{\partial z^*} dz^* + \frac{\partial P^*}{\partial r^*} dr^* \tag{28}$$

along any path starting at $z^* = 0$ and ending at $z^* = \frac{1}{2}$. From the equations of motion for creeping flow, we have

$$\frac{\partial P^*}{\partial r^*} = \frac{1}{N_{Re}} \left\{ \frac{\partial}{\partial r^*}\left[\frac{1}{r^*}\frac{\partial}{\partial r^*}(r^* v_r^*)\right] + \frac{\partial^2 v_r^*}{\partial {z^*}^2} \right\} \tag{29}$$

$$\frac{\partial P^*}{\partial z^*} = \frac{1}{N_{Re}} \left\{ \frac{1}{r^*}\frac{\partial}{\partial r^*}\left(r^* \frac{\partial v_z^*}{\partial r^*}\right) + \frac{\partial^2 v_z^*}{\partial {z^*}^2} \right\} \tag{30}$$

These equations can be expressed in terms of ψ_N^* and its derivatives (see also Neira, 1977) allowing in this way the evaluation of the pressure gradient at any point. Calculations can be carried out along different paths, such as along lines z^*, r^*, or ξ = constant. Using a finite-difference integration scheme, values of the pressure at a network of points can easily be obtained. Thus, in addition to the calculation of ΔP^*_{vd}, the dimensionless pressure drop through half a tube segment along lines $\hat{r} = r^*/r_w^*$ = constant were computed. The latter pressure drop is denoted by $\Delta P^*_{\hat{r}}$ and is given by

$$\Delta P^*_{\hat{r}} = \int_0^{1/2} \left[\left(\frac{\partial P^*}{\partial z^*}\right)_{r^*} - \left(\frac{\partial P^*}{\partial r^*}\right)_{z^*} \frac{(\partial \hat{r}/\partial z^*)_{r^*}}{(\partial \hat{r}/\partial r^*)_{z^*}}\right]_{\hat{r}} dz^* \tag{31}$$

SAMPLE CALCULATIONS

In order to illustrate the use and performance of the collocation method, the solution for the flow in a periodically constricted tube with geometry corresponding to $r_1^* = 0.1760$ and $r_2^* = 0.3975$ is given below. This geometry was also treated in Payatakes et al. (1973*b*), and thus comparison between the two methods can be made. This geometry is typical of a unit cell of a packed bed of sand.

Table 3. Collocation Solution for Different Numbers of Collocation Points and $w = 1$. Dimensionless Axial Velocity and Pressure Drop for $r_1^* = 0.1760$ and $r_2^* = 0.3975$

	$v_z^*(0, z^*)$			$-\Delta P^*_{\hat{r}_i}$ for $\hat{r}_i$ = roots of $P_{10}^{(0,1)}(\hat{r})$				
$n_r = n_z$	$z^* = 0$	$z^* = \frac{1}{2}$	$-\Delta P^*_{vd}$	$\hat{r}_2$	$\hat{r}_4$	$\hat{r}_6$	$\hat{r}_8$	$\hat{r}_{10}$
0	2.026	0.784	61.568	64.57	62.79	60.00	60.49	63.45
Collocation points from Equation (21) and roots of $P_{n_r}^{(3,0)}$								
2	1.982	0.812	61.437	62.56	61.87	59.55	61.68	67.01
3	1.898	0.759	61.244	61.51	61.39	60.68	60.79	63.60
4	1.916	0.752	61.224	61.61	61.38	60.90	60.58	62.70
5	1.915	0.752	61.222	61.58	61.42	60.92	60.50	62.25
6	1.914	0.752	61.221	61.59	61.38	60.89	60.48	61.96
Collocation points from Equation (21), and $\xi_i = \xi_i \left[\frac{i}{(n_r+1)} r_w^*, z^* \right]^\dagger$ for $i = 1, \ldots, n_r$								
2	1.980	0.814	61.435	62.38	61.91	59.59	61.43	64.48
3	1.898	0.760	61.246	61.57	61.37	60.70	60.69	63.68
4	1.916	0.753	61.226	61.60	61.40	60.92	60.47	62.64
5	1.915	0.752	61.223	61.59	61.43	60.93	60.40	62.14
6	1.914	0.752	61.222	61.60	61.38	60.89	60.40	61.87

† Equidistant points in the ξ direction.

Choice of Adjustable Coordinate Parameter w

A reasonable choice of the parameter w is made by examining the behavior of the solution obtained from the initial guess ψ_o^* of the trial function, Equation (19). Such an approximate solution is very sensitive to the value of w, Figure 3. w is adjusted to that value for which the calculated rate of viscous dissipation based on ψ_o^* becomes minimum. This procedure was arrived at heuristically by considering the classic theorem of Helmholtz (Lamb, 1932), which, of course, applies rigorously only to the exact solution. In practice, this criterion is applied by comparing the values of ΔP^*_{vd} obtained from ψ_o^* for different values of w. For most geometries of interest in modeling granular porous media, a minimum ΔP^*_{vd} is obtained for $w \approx 1$, Figure 4.

In addition to the previous analysis, calculations of the pressure drop by integration of the equations of motion along lines $\hat{r}$ = constant were carried out. It was found that for w values close to unity, the values of ΔP_r^* along different lines deviated less from the average value in the sense that the quantity

$$\{\text{Sum of squared differences}\} = \sum_{i=1}^{m} (\langle \Delta P^*_{r_i} \rangle - \Delta P^*_{r_i})^2$$

becomes minimum, Figure 4. This is as it should be, since we expect from the exact solution that ΔP_r^* = constant at $z^* = \frac{1}{2}$ for all $\hat{r}$.

Collocation solution

Based on the same criteria used in the adjustment of w, the convergence of the complete trial function was tested for an increasing number of collocation points. Approximate solutions were computed with w equal unity and selecting the roots of $P_{n_r}^{(3,0)}(\xi)$ as collocation abscissas. Some of the results are given in Table 1. These results show that for $n_r = n_z \geq 4$, the solutions for the stream function, velocity components, and pressure drop remain almost unchanged. The values of the pressure drops calculated along lines $\hat{r}$ = constant deviate by less than 1% from the average value, which in turn differs from ΔP^*_{vd} by about 0.3%. Almost identical results were obtained for values of w in the range 0.5 to 1.5, Table 2, and for other selections of the collocation abscissas, such as the roots

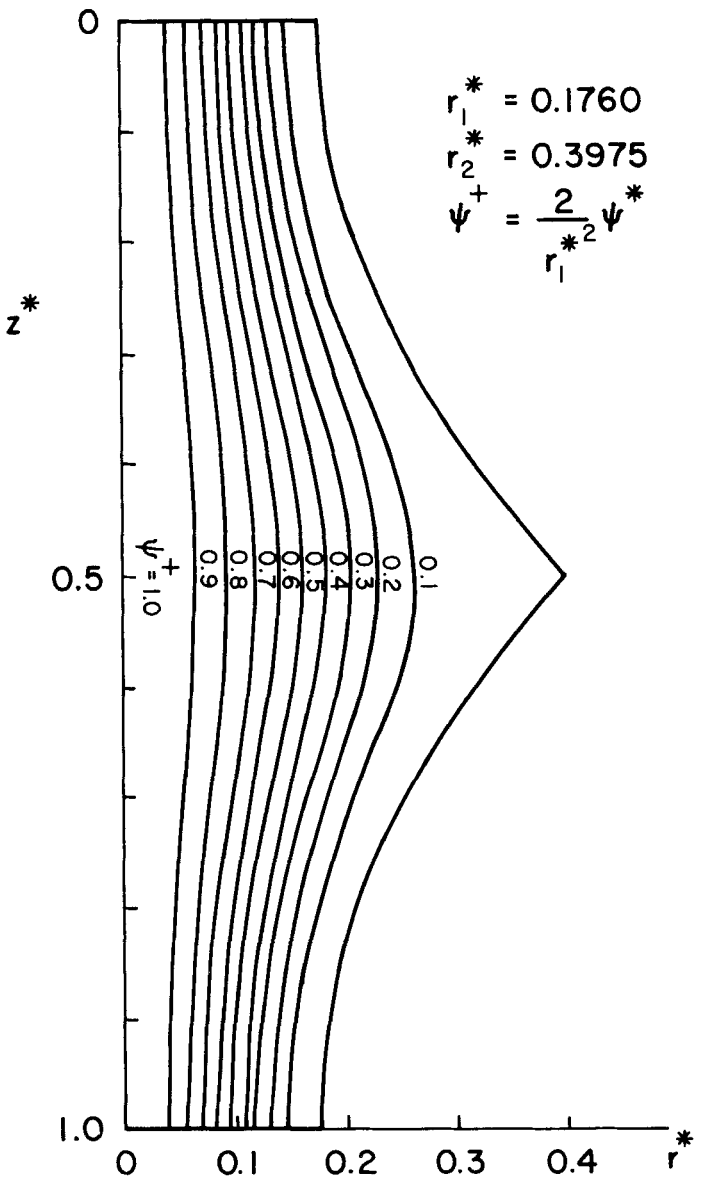

Fig. 5. Collocation solution with $w = 1$, $n_r = n_z = 4$ and collocation points on ξ from $P_4^{(3,0)}(\xi)$. Normalized stream function.

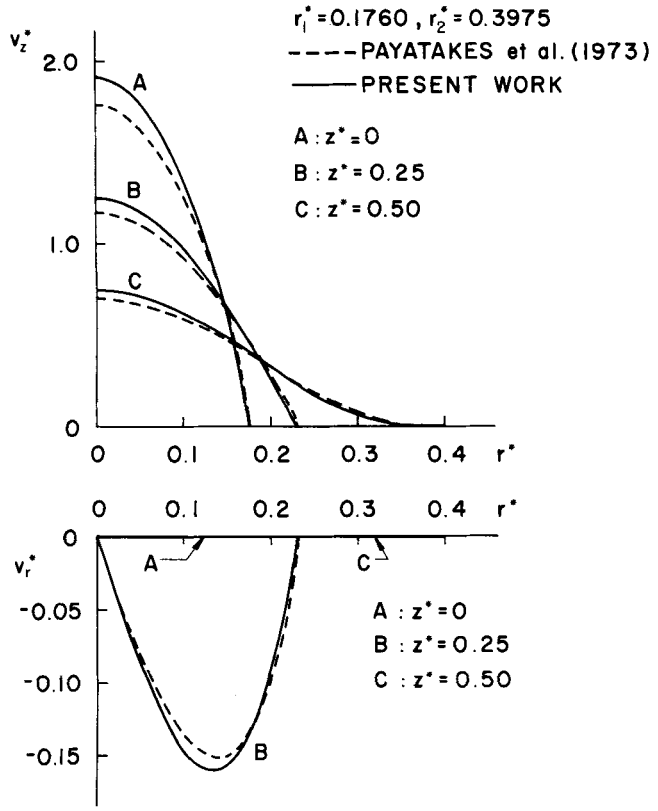

Fig. 6. Collocation solution with $w = 1$, $n_r = n_z = 4$ and collocation points on ξ from $P_4^{(3,0)}$ (ξ). Axial and radial dimensionless velocity profiles.

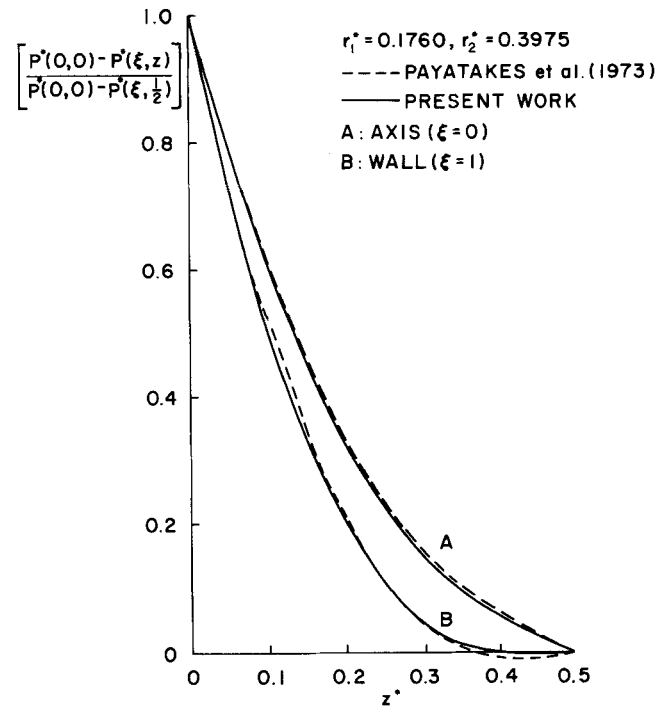

Fig. 7. Collocation solution with $w = 1$, $n_r = n_z = 4$ and collocation points on ξ from $P_4^{(3,0)}$ (ξ). Normalized pressure on the axis and on the wall.

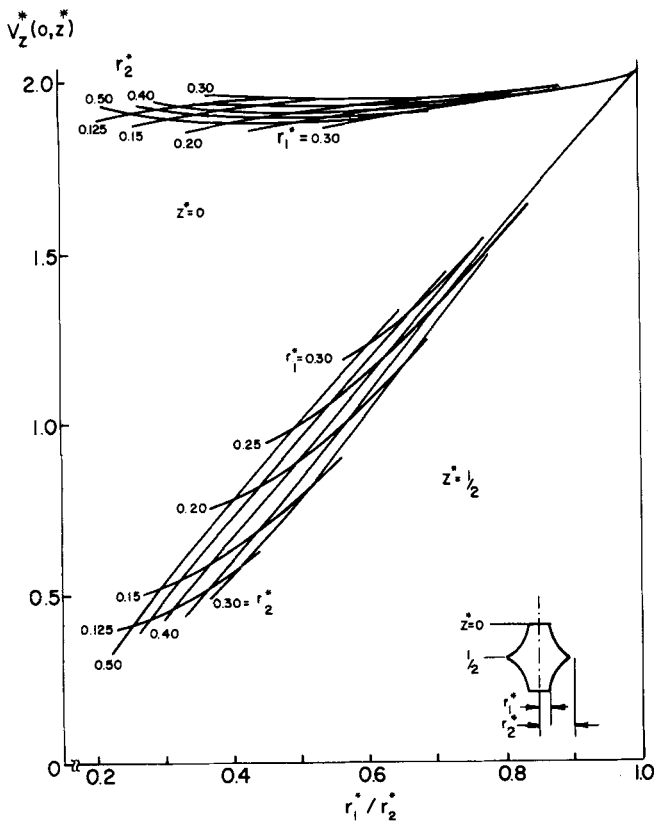

Fig. 8. Collocation solution for periodically constricted tubes of different geometries. Dimensionless axial velocity along the axis ($r^* = 0$).

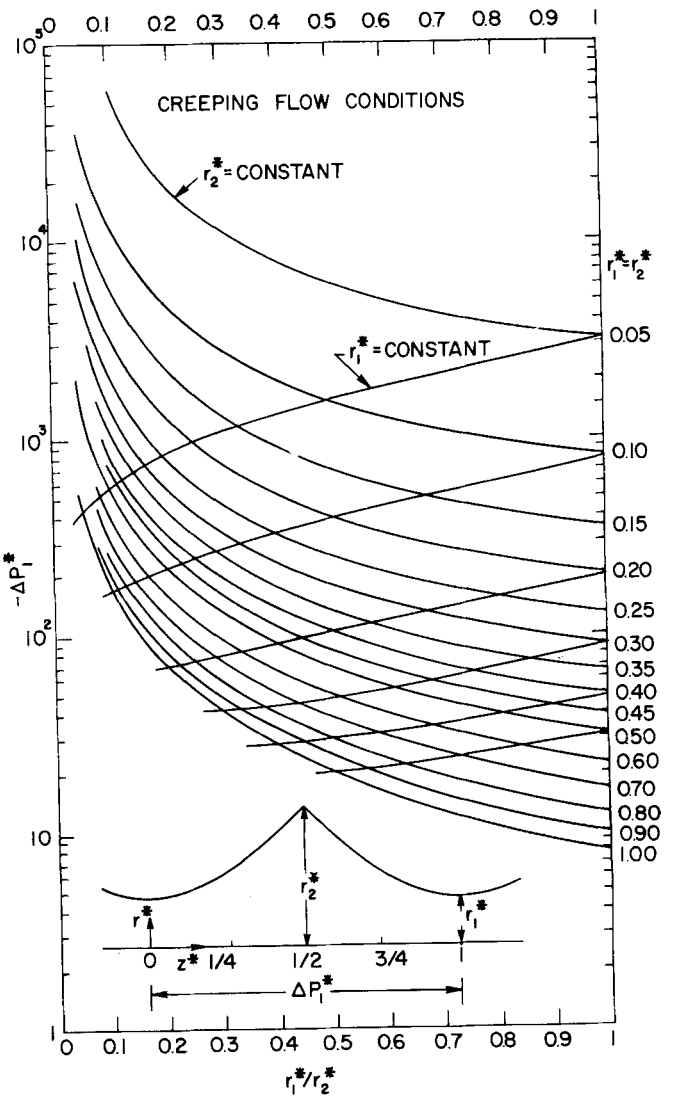

Fig. 9. Collocation solution for periodically constricted tubes of different geometries. Dimensionless pressure drop along one tube segment at $N_{Re} = 1$ (neglecting inertial effects).

TABLE 4. VALUES OF C_k FOR TUBES OF VARIOUS GEOMETRIES. $N = 16$ ($n_r = n_z = 4$)
COLLOCATION POINTS WERE USED, UNLESS OTHERWISE NOTED

k \ r_1^*	r_2^*	0.10				
		0.30	0.35	0.40	0.45	0.50
1		$-.27180 \times 10^{-5}$	$-.75605 \times 10^{-3}$	$-.10813 \times 10^{-2}$	$-.96980 \times 10^{-3}$	$-.55035 \times 10^{-3}$
2		$.24507 \times 10^{-3}$	$.72331 \times 10^{-3}$	$-.85861 \times 10^{-4}$	$-.20663 \times 10^{-2}$	$-.46409 \times 10^{-2}$
3		$-.32187 \times 10^{-3}$	$-.61919 \times 10^{-3}$	$.23578 \times 10^{-3}$	$.20330 \times 10^{-2}$	$.40753 \times 10^{-2}$
4		$.11596 \times 10^{-3}$	$.17620 \times 10^{-3}$	$-.15927 \times 10^{-3}$	$-.80756 \times 10^{-3}$	$-.15176 \times 10^{-2}$
5		$.84662 \times 10^{-3}$	$.30083 \times 10^{-2}$	$.44589 \times 10^{-2}$	$.50870 \times 10^{-2}$	$.50789 \times 10^{-2}$
6		$-.80274 \times 10^{-3}$	$-.24444 \times 10^{-2}$	$-.21895 \times 10^{-2}$	$-.14631 \times 10^{-3}$	$.27687 \times 10^{-2}$
7		$.70053 \times 10^{-3}$	$.15584 \times 10^{-2}$	$.70272 \times 10^{-3}$	$-.14695 \times 10^{-2}$	$-.37766 \times 10^{-2}$
8		$-.22647 \times 10^{-3}$	$-.39953 \times 10^{-3}$	$.11364 \times 10^{-4}$	$.82380 \times 10^{-3}$	$.15967 \times 10^{-2}$
9		$.86081 \times 10^{-3}$	$.36823 \times 10^{-3}$	$.43536 \times 10^{-3}$	$.10540 \times 10^{-2}$	$.20048 \times 10^{-2}$
10		$.35243 \times 10^{-3}$	$.96388 \times 10^{-3}$	$-.76075 \times 10^{-4}$	$-.23918 \times 10^{-2}$	$-.50564 \times 10^{-2}$
11		$-.45705 \times 10^{-3}$	$-.67183 \times 10^{-3}$	$.53514 \times 10^{-3}$	$.25726 \times 10^{-2}$	$.43386 \times 10^{-2}$
12		$.14679 \times 10^{-3}$	$.17320 \times 10^{-3}$	$-.21528 \times 10^{-3}$	$-.76815 \times 10^{-3}$	$-.10804 \times 10^{-2}$
13		$-.74057 \times 10^{-4}$	$.35436 \times 10^{-3}$	$.56540 \times 10^{-3}$	$.57527 \times 10^{-3}$	$.51179 \times 10^{-2}$
14		$-.41532 \times 10^{-3}$	$-.10351 \times 10^{-2}$	$-.10796 \times 10^{-2}$	$-.85104 \times 10^{-3}$	$-.86464 \times 10^{-3}$
15		$.28066 \times 10^{-3}$	$.48022 \times 10^{-3}$	$.31202 \times 10^{-3}$	$.26256 \times 10^{-3}$	$.93335 \times 10^{-3}$
16		$-.75938 \times 10^{-4}$	$-.13355 \times 10^{-3}$	$-.15796 \times 10^{-3}$	$-.35876 \times 10^{-3}$	$-.95519 \times 10^{-3}$

k \ r_1^*	r_2^*	0.20				
		0.30#	0.35	0.40	0.45	0.50
1		$.30660 \times 10^{-1}$	$.96522 \times 10^{-2}$	$.19752 \times 10^{-2}$	$-.38070 \times 10^{-2}$	$-.76848 \times 10^{-2}$
2		$-.10442$	$-.10185 \times 10^{-1}$	$-.44059 \times 10^{-3}$	$.55407 \times 10^{-2}$	$.70222 \times 10^{-2}$
3		$.31466$	$.74916 \times 10^{-2}$	$.10465 \times 10^{-3}$	$-.41516 \times 10^{-2}$	$-.45379 \times 10^{-2}$
4		$-.65475$	$-.22678 \times 10^{-2}$	$.22638 \times 10^{-5}$	$.12869 \times 10^{-2}$	$.13164 \times 10^{-2}$
5		$.88465$	$-.11387 \times 10^{-1}$	$-.20651 \times 10^{-2}$	$.65435 \times 10^{-2}$	$.12910 \times 10^{-1}$
6		$-.73787$	$.16856 \times 10^{-1}$	$.11204 \times 10^{-2}$	$-.94117 \times 10^{-2}$	$-.12252 \times 10^{-1}$
7		$.34420$	$-.13023 \times 10^{-1}$	$-.26864 \times 10^{-3}$	$.74767 \times 10^{-2}$	$.81196 \times 10^{-2}$
8		$-.68566 \times 10^{-1}$	$.39913 \times 10^{-2}$	$-.81898 \times 10^{-5}$	$-.23349 \times 10^{-2}$	$-.22906 \times 10^{-2}$
9		$-.35878 \times 10^{-1}$	$.56123 \times 10^{-2}$	$.25863 \times 10^{-2}$	$-.36810 \times 10^{-3}$	$-.18215 \times 10^{-2}$
10		$.16720$	$-.10310 \times 10^{-1}$	$-.13318 \times 10^{-2}$	$.56844 \times 10^{-2}$	$.74193 \times 10^{-2}$
11		$-.52787$	$.84824 \times 10^{-2}$	$.21827 \times 10^{-3}$	$-.52739 \times 10^{-2}$	$-.53482 \times 10^{-2}$
12		$.11093 \times 10$	$-.26609 \times 10^{-2}$	$.37420 \times 10^{-4}$	$.16463 \times 10^{-2}$	$.13770 \times 10^{-2}$
13		$-.15031 \times 10$	$-.17539 \times 10^{-2}$	$-.55679 \times 10^{-3}$	$.85011 \times 10^{-3}$	$.16901 \times 10^{-2}$
14		$.12550 \times 10$	$.40674 \times 10^{-2}$	$.37005 \times 10^{-3}$	$-.28482 \times 10^{-2}$	$-.37120 \times 10^{-2}$
15		$-.58568$	$-.35779 \times 10^{-2}$	$.47157 \times 10^{-4}$	$.23839 \times 10^{-2}$	$.20279 \times 10^{-2}$
16		$.11669$	$.11483 \times 10^{-2}$	$-.58734 \times 10^{-4}$	$-.68624 \times 10^{-3}$	$-.41983 \times 10^{-3}$
17		$.15122 \times 10^{-1}$				
18		$-.85584 \times 10^{-1}$				
19		$.28344$				
20		$-.60345$				
21		$.82099$				
22		$-.68636$				
23		$.32041$				
24		$-.63839 \times 10^{-1}$				
25						
26						
27						
28						

(Continued on page 51)

of $P_{n_r}^{(3,1)}$ and $P_{n_r}^{(1,0)}$, and the equidistant points on r^*/r_w^*, Table 3.

Figures 5 to 7 show the solutions obtained for the streamlines, axial, and radial velocity profiles and normalized pressure profiles for the sample case. These results were obtained by using $w = 1$, $n_r = n_z = 4$, and the roots of $P_{n_r}^{(3,0)}(\xi)$ as collocation abscissas. Together with the present results, these figures show the profiles obtained by Payatakes et al. (1973*b*). Their solution was obtained using a finite-difference network containing approximately 350 nodes in the region $0 \leq z^* \leq \frac{1}{2}$. As can be seen, the largest differences between both approximations are found in the velocity profiles. The solution of Payatakes et al. for the axial velocity along the axis and the radial velocity at $z^* = 0.25$ (where the largest values are found) differs by about -8% from the values given by the present work. For the pressure drop, that difference is -4.7%. Most of this discrepancy is most likely due to discretization error in the finite-difference solution.

GENERAL RESULTS

Calculations were carried out for various tube geometries with parameters in the ranges $0.125 \leq r_1^* \leq 0.3$ and $0.3 \leq r_2^* \leq 0.5$. It is estimated that these values should contain the range of unit cell geometries postulated in the models by Payatakes, Tien, and Turian (1973*a*) and Payatakes and Neira (1977). The collocation expansion coefficients C_k are given in Table 4. The calculated pressure drop ($-\Delta P_1^*$) and the axial velocity values at $z^* =$

TABLE 4. (cont'd.)

k \ r_1^* / r_2^*	0.125				
	0.30	0.35	0.40	0.45	0.50
1	$.95643 \times 10^{-3}$	$-.86723 \times 10^{-3}$	$-.20593 \times 10^{-2}$	$-.25027 \times 10^{-2}$	$-.22422 \times 10^{-2}$
2	$-.90175 \times 10^{-3}$	$.12211 \times 10^{-2}$	$.16502 \times 10^{-2}$	$.42621 \times 10^{-4}$	$-.32628 \times 10^{-2}$
3	$.58027 \times 10^{-3}$	$-.10526 \times 10^{-2}$	$-.11871 \times 10^{-2}$	$.43280 \times 10^{-3}$	$.33972 \times 10^{-2}$
4	$-.15565 \times 10^{-3}$	$.33959 \times 10^{-3}$	$.32439 \times 10^{-3}$	$-.28231 \times 10^{-3}$	$-.12880 \times 10^{-2}$
5	$-.14572 \times 10^{-2}$	$.22294 \times 10^{-2}$	$.51157 \times 10^{-2}$	$.67898 \times 10^{-2}$	$.72386 \times 10^{-2}$
6	$.16356 \times 10^{-2}$	$-.24863 \times 10^{-2}$	$-.39207 \times 10^{-2}$	$-.21513 \times 10^{-2}$	$.21894 \times 10^{-2}$
7	$-.10158 \times 10^{-2}$	$.19926 \times 10^{-2}$	$.23894 \times 10^{-2}$	$-.35910 \times 10^{-4}$	$-.42202 \times 10^{-2}$
8	$.26889 \times 10^{-3}$	$-.61749 \times 10^{-3}$	$-.59265 \times 10^{-3}$	$.37591 \times 10^{-3}$	$.18546 \times 10^{-2}$
9	$.18747 \times 10^{-2}$	$.60714 \times 10^{-3}$	$.71433 \times 10^{-5}$	$.33140 \times 10^{-3}$	$.14849 \times 10^{-2}$
10	$-.12436 \times 10^{-2}$	$.15532 \times 10^{-2}$	$.20322 \times 10^{-2}$	$-.43239 \times 10^{-4}$	$-.38942 \times 10^{-2}$
11	$.65902 \times 10^{-3}$	$-.13949 \times 10^{-2}$	$-.12378 \times 10^{-2}$	$.10348 \times 10^{-2}$	$.43076 \times 10^{-2}$
12	$-.16833 \times 10^{-3}$	$.41397 \times 10^{-3}$	$.27724 \times 10^{-3}$	$-.46196 \times 10^{-3}$	$-.13465 \times 10^{-2}$
13	$-.56301 \times 10^{-3}$	$.18145 \times 10^{-3}$	$.67841 \times 10^{-3}$	$.82221 \times 10^{-3}$	$.70359 \times 10^{-3}$
14	$.49657 \times 10^{-3}$	$-.10143 \times 10^{-2}$	$-.15369 \times 10^{-2}$	$-.12072 \times 10^{-2}$	$-.64281 \times 10^{-3}$
15	$-.24582 \times 10^{-3}$	$.68004 \times 10^{-3}$	$.61319 \times 10^{-3}$	$.47954 \times 10^{-4}$	$-.13690 \times 10^{-3}$
16	$.65116 \times 10^{-4}$	$-.17925 \times 10^{-3}$	$-.15003 \times 10^{-3}$	$-.10235 \times 10^{-3}$	$-.39399 \times 10^{-3}$

k \ r_1^* / r_2^*	0.25				
	0.30##	0.35#	0.40	0.45	0.50
1	.19481	$.62275 \times 10^{-1}$	$.20469 \times 10^{-1}$	$.64391 \times 10^{-2}$	$-.41857 \times 10^{-2}$
2	$-.18902 \times 10$	$-.22669$	$-.21355 \times 10^{-1}$	$-.26334 \times 10^{-2}$	$.90533 \times 10^{-2}$
3	$.16175 \times 10^{2}$	.70424	$.15372 \times 10^{-1}$	$.13193 \times 10^{-2}$	$-.68883 \times 10^{-2}$
4	$-.10376 \times 10^{3}$	$-.14941 \times 10$	$-.46143 \times 10^{-2}$	$-.34116 \times 10^{-3}$	$.21100 \times 10^{-2}$
5	$.48526 \times 10^{3}$	$.20445 \times 10$	$-.18439 \times 10^{-1}$	$-.46317 \times 10^{-2}$	$.87801 \times 10^{-2}$
6	$-.16600 \times 10^{4}$	$-.17198 \times 10$	$.30609 \times 10^{-1}$	$.44670 \times 10^{-2}$	$-.14595 \times 10^{-1}$
7	$.41814 \times 10^{4}$	.80694	$-.24412 \times 10^{-1}$	$-.26000 \times 10^{-2}$	$.11840 \times 10^{-1}$
8	$-.77787 \times 10^{4}$	$-.16142$	$.75681 \times 10^{-2}$	$.66973 \times 10^{-3}$	$-.37324 \times 10^{-2}$
9	$.10643 \times 10^{5}$	$-.62941 \times 10^{-1}$	$.72406 \times 10^{-2}$	$.36464 \times 10^{-2}$	$-.61377 \times 10^{-3}$
10	$-.10562 \times 10^{5}$	.33879	$-.15367 \times 10^{-1}$	$-.38201 \times 10^{-2}$	$.73901 \times 10^{-2}$
11	$.73887 \times 10^{4}$	$-.11389 \times 10$	$.13472 \times 10^{-1}$	$.21042 \times 10^{-2}$	$-.76251 \times 10^{-2}$
12	$-.34518 \times 10^{4}$	$.24700 \times 10$	$-.43613 \times 10^{-2}$	$-.50993 \times 10^{-3}$	$.25415 \times 10^{-2}$
13	$.96604 \times 10^{3}$	$-.34074 \times 10$	$-.18945 \times 10^{-2}$	$-.79221 \times 10^{-3}$	$.98877 \times 10^{-3}$
14	$-.12244 \times 10^{3}$	$.28769 \times 10$	$.49855 \times 10^{-2}$	$.11980 \times 10^{-2}$	$-.35401 \times 10^{-2}$
15	$-.15554$	$-.13526 \times 10$	$-.47673 \times 10^{-2}$	$-.70057 \times 10^{-3}$	$.34247 \times 10^{-2}$
16	$.22237 \times 10$	.27089	$.16079 \times 10^{-2}$	$.16502 \times 10^{-3}$	$-.10950 \times 10^{-2}$
17	$-.20969 \times 10^{2}$	$.24350 \times 10^{-1}$			
18	$.13886 \times 10^{3}$	$-.16153$			
19	$-.65799 \times 10^{3}$	.58015			
20	$.22652 \times 10^{4}$	$-.12886 \times 10$			
21	$-.57262 \times 10^{4}$	$.17954 \times 10$			
22	$.10675 \times 10^{5}$	$-.15231 \times 10$			
23	$-.14626 \times 10^{5}$	.71789			
24	$.14529 \times 10^{5}$	$-.14398$			
25	$-.10171 \times 10^{5}$				
26	$.47538 \times 10^{4}$				
27	$-.13309 \times 10^{4}$				
28	$.16874 \times 10^{3}$				

(Continued on opposite page)

0, ½ are listed in Table 5. Figures 8 and 9 summarize some significant results. Figure 8 shows the calculated dimensionless axial velocity along the axis at $z^* = 0$ and $z^* = ½$ and Figure 9 the calculated dimensionless pressure drop through a single segment at $N_{Re} = 1$, neglecting inertial effects. The reported values for the pressure drop were obtained from the integration of the rate of viscous dissipation. These values were found to converge slightly faster than those calculated by path integration of the Navier-Stokes equations. The curves in Figure 9 are in excellent agreement with the Hagen-Poiseuille solution (exact) for $r_1^*/r_2^* = 1$.

The choices of w and collocation points used for the sample calculation were found appropriate for a wide range of geometries. Thus, for ratios r_1^*/r_2^* in the range 0.25 to 0.8, satisfactory convergence is achieved by using $w = 1$, $n_r = n_z = 4$, and the roots of $P_{n_r}^{(3,0)}(\xi)$ as collocation abscissas. As the ratio r_1^*/r_2^* approaches unity, the solution becomes less dependent on z^*, and consequently fewer collocation points along the z^* axis are needed. However, in order to obtain acceptable accuracy, it was necessary to increase the number of collocation points in the radial direction. This should be attributed to the fact that as r_1^*/r_2^* approaches unity, the initial guess ψ_o^* becomes quite different from the Hagen-Poiseuille solution, owing to the definition of ξ [Equation (15)]. This difficulty could be circumvented by changing the exponent p in the following expression

$$\psi_o^* = (r_1^{*2}/2)(1 - \xi)^p \qquad (32)$$

from $p = 2$ [see Equation (19)] to $p = 1$, which is the Hagen-Poiseuille solution. However, the choice $p = 1$ is

TABLE 4. (cont'd.)

k \ r_1^*	r_2^*	0.15				
		0.30	0.35	0.40	0.45	0.50
1		$.37065 \times 10^{-2}$	$.20817 \times 10^{-3}$	$-.23923 \times 10^{-2}$	$-.39673 \times 10^{-2}$	$-.44154 \times 10^{-2}$
2		$-.41736 \times 10^{-2}$	$.27044 \times 10^{-3}$	$.27888 \times 10^{-2}$	$.26654 \times 10^{-2}$	$-.31737 \times 10^{-3}$
3		$.31112 \times 10^{-2}$	$-.34086 \times 10^{-3}$	$-.21470 \times 10^{-2}$	$-.16475 \times 10^{-2}$	$.12142 \times 10^{-2}$
4		$-.93991 \times 10^{-3}$	$.13361 \times 10^{-3}$	$.66563 \times 10^{-3}$	$.42313 \times 10^{-3}$	$-.59714 \times 10^{-3}$
5		$-.56290 \times 10^{-2}$	$-.17887 \times 10^{-3}$	$.46548 \times 10^{-2}$	$.80651 \times 10^{-2}$	$.96584 \times 10^{-2}$
6		$.74816 \times 10^{-2}$	$-.41481 \times 10^{-3}$	$-.51963 \times 10^{-2}$	$-.55332 \times 10^{-2}$	$-.12009 \times 10^{-2}$
7		$-.56152 \times 10^{-2}$	$.66752 \times 10^{-3}$	$.39373 \times 10^{-2}$	$.30492 \times 10^{-2}$	$-.17898 \times 10^{-2}$
8		$.16963 \times 10^{-2}$	$-.26198 \times 10^{-3}$	$-.11871 \times 10^{-2}$	$-.69426 \times 10^{-3}$	$.10841 \times 10^{-2}$
9		$.35905 \times 10^{-2}$	$.15948 \times 10^{-2}$	$.42937 \times 10^{-5}$	$-.48595 \times 10^{-3}$	$.35148 \times 10^{-3}$
10		$-.52491 \times 10^{-2}$	$.13098 \times 10^{-3}$	$.33475 \times 10^{-2}$	$.30506 \times 10^{-2}$	$-.72476 \times 10^{-3}$
11		$.39757 \times 10^{-2}$	$-.58280 \times 10^{-3}$	$-.27262 \times 10^{-2}$	$-.15741 \times 10^{-2}$	$.23332 \times 10^{-2}$
12		$-.12002 \times 10^{-2}$	$.22273 \times 10^{-3}$	$.77794 \times 10^{-3}$	$.26686 \times 10^{-3}$	$-.10009 \times 10^{-2}$
13		$-.12642 \times 10^{-2}$	$-.29280 \times 10^{-3}$	$.60355 \times 10^{-3}$	$.10637 \times 10^{-2}$	$.10363 \times 10^{-2}$
14		$.23684 \times 10^{-2}$	$-.22698 \times 10^{-3}$	$-.18651 \times 10^{-2}$	$-.20127 \times 10^{-2}$	$-.10940 \times 10^{-2}$
15		$-.18322 \times 10^{-2}$	$.36691 \times 10^{-3}$	$.12016 \times 10^{-2}$	$.61991 \times 10^{-3}$	$-.47865 \times 10^{-3}$
16		$.55258 \times 10^{-3}$	$-.11866 \times 10^{-3}$	$-.30355 \times 10^{-3}$	$-.11325 \times 10^{-3}$	$.28755 \times 10^{-4}$

k \ r_1^*	r_2^*	0.30			
		0.35##	0.40#	0.45	0.50
1		.35018	.10987	$.37645 \times 10^{-1}$	$.14855 \times 10^{-1}$
2		$-.37866 \times 10$	$-.41976$	$-.40465 \times 10^{-1}$	$-.78313 \times 10^{-2}$
3		$.34019 \times 10^{2}$	$.13212 \times 10$	$.28822 \times 10^{-1}$	$.41558 \times 10^{-2}$
4		$-.22376 \times 10^{3}$	$-.28228 \times 10$	$-.85829 \times 10^{-2}$	$-.11083 \times 10^{-2}$
5		$.10619 \times 10^{4}$	$.38807 \times 10$	$-.26007 \times 10^{-1}$	$-.76059 \times 10^{-2}$
6		$-.36658 \times 10^{4}$	$-.32749 \times 10$	$.47839 \times 10^{-1}$	$.99354 \times 10^{-2}$
7		$.92911 \times 10^{4}$	$.15402 \times 10$	$-.39565 \times 10^{-1}$	$-.68400 \times 10^{-2}$
8		$-.17359 \times 10^{5}$	$-.30862$	$.12448 \times 10^{-1}$	$.19497 \times 10^{-2}$
9		$.23827 \times 10^{5}$	$-.95749 \times 10^{-1}$	$.81777 \times 10^{-2}$	$.45855 \times 10^{-2}$
10		$-.23702 \times 10^{5}$	$.57074$	$-.19167 \times 10^{-1}$	$-.67818 \times 10^{-2}$
11		$.16610 \times 10^{5}$	$-.20046 \times 10$	$.17651 \times 10^{-1}$	$.47753 \times 10^{-2}$
12		$-.77711 \times 10^{4}$	$.44417 \times 10$	$-.58668 \times 10^{-2}$	$-.13626 \times 10^{-2}$
13		$.21774 \times 10^{4}$	$-.62011 \times 10$	$-.17342 \times 10^{-2}$	$-.93005 \times 10^{-3}$
14		$-.27623 \times 10^{3}$	$.52743 \times 10$	$.49394 \times 10^{-2}$	$.19034 \times 10^{-2}$
15		$-.25289$	$-.24917 \times 10$	$-.49861 \times 10^{-2}$	$-.15024 \times 10^{-2}$
16		$.40967 \times 10$	$.50071$	$.17419 \times 10^{-2}$	$.44669 \times 10^{-3}$
17		$-.41224 \times 10^{2}$	$.33462 \times 10^{-1}$		
18		$.28282 \times 10^{3}$	$-.24752$		
19		$-.13683 \times 10^{4}$	$.94119$		
20		$.47723 \times 10^{4}$	$-.21562 \times 10$		
21		$-.12169 \times 10^{5}$	$.30593 \times 10$		
22		$.22824 \times 10^{5}$	$-.26249 \times 10$		
23		$-.31410 \times 10^{5}$	$.12466 \times 10$		
24		$.31303 \times 10^{5}$	$-.25135$		
25		$-.21968 \times 10^{5}$			
26		$.10288 \times 10^{5}$			
27		$-.28850 \times 10^{4}$			
28		$.36623 \times 10^{3}$			

(#) $N = 24$ ($n_r = 8$, $n_z = 3$) collocation points.
(##) $N = 28$ ($n_r = 12$, $n_z = 2$) collocation points.

only admissible for $r_1^* = r_2^*$. For any other case, it results in inability to satisfy the no-slip condition on the tube wall.*

* This situation does not arise when ξ is defined by $\xi = r/r_w(z)$, as in Fedkiw and Newman (1977) and Neira and Payatakes (1978). However, if the latter transformation is used when the wall has a cusp at $z^\circ = \frac{1}{2}$, v_r° does not vanish automatically on the plane $z^\circ = \frac{1}{2}$, as it ought to do. As a partial remedy, the radial velocity can be forced to vanish at a number of collocation points on $z^\circ = \frac{1}{2}$. This generates an extra set of equations to be used as boundary conditions in the collocation solution.

The use of Equation (15), on the other hand, eliminates this need since then v_r° vanishes automatically everywhere on $z^\circ = 0$ and $z^\circ = \frac{1}{2}$. Actually, even the limiting behavior as $r_1^\circ \to r_2^\circ$ does not really present a problem since in practice the amplitude is always finite, usually sizable. If $r_1^\circ = r_2^\circ$, the solution is the Hagen-Poiseuille flow, and the collocation is completely unnecessary.

The present solution was compared with the finite-difference solution of Payatakes et al. (1973*b*) by making the calculations for the geometries reported in Table 4.1 of Payatakes (1973). The dimensionless pressure drop values in Payatakes (1973) were obtained using a network step increment of 1/36; the values from the present solution were obtained using $w = 1$, $n_r = n_z = 4$, and the roots of $P_{n_r}^{(3,0)}(\xi)$ as collocation abscissas.

In the range $\{r_1^* = 0.3;\ 0.35 \leq r_2^* \leq 0.5\}$, the $(-\Delta P_1^*)$ values from the finite-difference solution are -3 to -4% smaller than those from the collocation solution. In the range $\{r_1^* = 0.24;\ 0.35 \leq r_2^* \leq 0.5\}$, the difference becomes -5 to -6%. These differences are to be expected and they are due to discretization errors

TABLE 5. COLLOCATION SOLUTION FOR PERIODICALLY CONSTRICTED TUBES OF DIFFERENT GEOMETRIES USING $w = 1$, $n_r = n_z = 4$, AND THE ROOTS OF $P_4^{(3,0)}(\xi)$ AS COLLOCATION ABSCISSAS. DIMENSIONLESS AXIAL VELOCITY ALONG THE AXIS AND PRESSURE DROP

THE ENTRIES ARE:
1) $-\Delta P_1^* = -2\Delta P^*_{vd}$
2) $v_z^*(0, 0)$
3) $v_z^*(0, \frac{1}{2})$

r_2^*	r_1^* 0.125	0.15	0.20	0.25	0.30
	222.9	179.0	129.6	104.0†	88.89††
0.30	1.952	1.949	1.952	1.978	2.000
	0.587	0.775	1.192	1.609	2.000
	202.2	161.3	114.3	89.41	74.47
0.35	1.941	1.934	1.932	1.942	1.969
	0.509	0.666	0.996	1.357	1.679
	187.3	148.8	104.3	80.05	65.65
0.40	1.930	1.921	1.913	1.917	1.934
	0.460	0.601	0.886	1.173	1.484
	176.0	139.5	97.20	73.87	59.43
0.45	1.921	1.909	1.897	1.896	1.904
	0.427	0.557	0.818	1.068	1.213
	167.0	132.2	91.82	69.40	55.35
0.50	1.915	1.899	1.882	1.877	1.880
	0.402	0.526	0.773	1.005	1.217

† Obtained with $n_z = 2$ and $n_r = 14$.
†† Hagen-Poiseuille solution.

in the finite-difference solutions. Since the finite difference values were obtained with a constant step increment, their accuracy is expected to improve as the values of r_1^* and r_2^* increase. Payatakes et al. (1976*b*) estimated differences of about -3.5% from the exact solution in cases when a finite-difference network containing at least fourteen nodes on each row was used. Approximately, this situation corresponds to the case $r_1^* = 0.3$, $(r_2^* > 0.3)$. The agreement between the deviations from the collocation solution and those from the exact solution is rather remarkable. This demonstrates the high accuracy which is achieved with the collocation solution.

NOTATION

C_k = expansion coefficients, Equation (18)
g = gravitational acceleration
h = length of one segment of a periodically constricted tube
i, j, k = indexes
N = total number of interior collocation points
n_r, n_z = number of radial and axial expansion functions (or collocation points)
N_{Re} = Reynolds number, Equation (6)
p = thermodynamic pressure
P = total pressure (including hydrostatic pressure)
P^* = dimensionless pressure, Equation (5)
$P_n^{(\alpha,\beta)}$ = Jacobi polynomial, Equation (22) and Appendix B
q = volumetric flow rate
$R(\xi, \eta)$ = residual, Equation (20)
R_{ij} = residual at $\xi = \xi_i$, $\eta = \eta_j$
(r, θ, z) = cylindrical coordinates
(r^*, θ, z^*) = dimensionless cylindrical coordinates, Equation (1)
$r_w^*(z^*)$ = dimensionless wall radius, Equation (2)
r_1^*, r_2^* = dimensionless minimum and maximum wall radii
$\hat{r}$ = normalized radial coordinate, r^*/r_w^*
$\hat{r}_{ij}$ = values of $\hat{r}$ corresponding to the roots of $P_m^{(0,1)}[\hat{r}(z_j^*)]$, Equation (27)
v_o = mean velocity at a cross section of minimum radius, Equation (3)
v_r, v_z = velocity components
v_r^*, v_z^* = dimensionless velocity components, Equation (4)
V^* = dimensionless volume of integration region
w = free parameter of coordinate system (ξ, η) Equation (17)
z_j^* = roots of the Jacobi polynomial $P_n^{(0,0)}(2z^*)$, Equation (27)

Greek Letters

γ = function defined by Equation (17)
ΔP^* = dimensionless pressure drop along one tube segment
ΔP^*_{vd}, $\Delta P^*_{\hat{r}}$ = values of dimensionless pressure drop along half a tube segment calculated from viscous dissipation, and by integration of the equations of motion along a line $\hat{r}$ = constant, respectively
$\Delta P^*_{\hat{r}_i}$ = value of ΔP_r^* at $\hat{r} = \hat{r}_i$
η = new axial coordinate, Equation (16)
η_i = value of η at the i^{th} axial collocation point
μ = viscosity
ξ = new radial coordinate, Equation (15)
ξ_j = value of ξ at the j^{th} radial collocation point
ρ = fluid density
Φ_v^* = dimensionless viscous dissipation function, Equation (26)
ψ = stream function
ψ^* = dimensionless stream function, Equation (7)
ψ_o^* = initial guess in trial function, Equation (19)
ψ_N^* = trial function, Equation (18)

LITERATURE CITED

Bird, R. B., W. E. Stewart, and E. N. Lightfoot, *Transport Phenomena*, Wiley, New York (1960).

Chow, J. C. F., and K. Soda, "Laminar Flow in Tubes with Constriction", *Phys. Fluids*, **15**, 1700 (1972).

Dodson, A. G., P. Townsend, and K. Walters, "On the Flow of Newtonian and Non-Newtonian Liquids Through Corrugated Pipes," *Rheol. Acta*, **10**, 508 (1971).

Fedkiw, P., and J. Newman, "Mass Transfer at High Peclet Numbers for Creeping Flow in a Packed Bed Reactor," *AIChE J.*, **23**, 255 (1977).

Houpeurt, A., "Sur l'Ecoulement des Gaz dans les Milieux Poreux," *Rev. Inst. Fr. Petrole Ann. Combust. Liquides*, **14**, 1468 (1959).

Ladyzhenskaya, O. A., "Mathematical Analysis of Navier-Stokes Equations for Incompressible Liquids," *Ann. Rev. Fluid Mech.*, **7**, 249 (1975).

Lamb, H, *Hydrodynamics*, Dover, New York (1932).

Neira, M. A., "A New Model of the Constricted Unit Cell Type for Granular Porous Media and Collocation Solution of the Creeping Newtonian Flow Problem," Master thesis, Univ. Houston, Tex. (1977).

———, and A. C. Payatakes, "Collocation Solution of Creeping Newtonian Flow through Sinusoidal Tubes," *AIChE J.*, **24**, (1978).

Oh, S. G., and J. C. Slattery, "Interfacial Tension Required for Significant Displacement of Oil," 2nd Annual Enhanced Oil and Gas Recovery Symposium, ERDA, Tulsa, Okla. (Sept., 1976).

Payatakes, A. C., "A New Model for Granular Porous Media. Application to Filtration Through Packed Beds," Doctoral dissertation, Syracuse Univ, N.Y. (1973).

———, and M. A. Neira, "Model of the Constricted Unit Cell Type for Isotropic Granular Porous Media," *AIChE J.*, **23**, 922 (1977).
Payatakes, A. C., D. H. Brown, and Chi Tien, "On the Transient Behavior of Deep Bed Filtration," AIChE 83rd National Meeting, Houston, Tex. (Mar., 1977).
Payatakes, A. C., Chi Tien, and R. M. Turian, "A New Model for Granular Porous Media. Part I. Model Formulation," *AIChE J.*, **19**, 58 (1973*a*).
———, "A New Model for Granular Porous Media. Part II. Numerical Solution of Steady State Incompressible Newtonian Flow through Periodically Constricted Tubes," *ibid.*, 67 (1973*b*).
———, "Further Work on the Flow Through Periodically Constricted Tubes—A Reply," *ibid.*, 1036 (1973*c*).
———, "Trajectory Calculation of Particle Deposition in Deep Bed Filtration. Part I. Model Formulation," *ibid.*, **20**, 889 (1947*a*).
———, "Trajectory Calculation of Particle Deposition in Deep Bed Filtration. Part II. Case Study of the Effect of the Dimensionless Groups and Comparison with Experimental Data," *ibid.*, 900 (1974*b*).
Petersen, E. E., "Diffusion in a Pore of Varying Cross Section," *ibid.*, **4**, 343 (1958).
Rajagopalan, R., and Chi Tien, "Trajectory Analysis of Deep-Bed Filtration with the Sphere-in-cell Porous Media Model," *ibid.*, **22**, 523 (1976).
Sheffield, R. E., and A. B. Metzner, "Flow of Non-linear Fluids Through Porous Media," *ibid.*, **22**, 736 (1976).
Slattery, J. C., "Interfacial Effects in the Entrapment and Displacement of Residual Oil," *ibid.*, **20**, 1145 (1974).
Stegermeier, G. L., "Mechanisms of Entrapment and Mobilization of Oil in Porous Medium," 81st AIChE Meeting, Kansas City, Mo. (Apr., 1976).
Villadsen, J., "Selected Approximation Methods for Chemical Engineering Problems," Inst. for Kemiteknik Numer. Inst. Danmarks Tekniske Højskole (1970).

APPENDIX A: EQUATION OF MOTION FOR CREEPING FLOW IN THE NEW SYSTEM OF COORDINATES

The fourth-order partial differential equation governing the flow, Equation (8), can be expressed in terms of the new coordinate system

$$\xi = \xi(r^*, z^*)$$

$$\eta = z^*$$

as follows:

$$E^{*4}\psi^* = \sum_{i=1}^{15} a_i T_i = 0$$

where a_i and T_i are given by

i	T_i	a_i
1	ψ^*	0
2	$\frac{\partial\psi^*}{\partial\xi}$	$-\frac{3}{r^{*3}}\frac{\partial\xi}{\partial r^*}+\frac{3}{r^{*2}}\frac{\partial^2\xi}{\partial r^{*2}}-\frac{2}{r^*}\frac{\partial^3\xi}{\partial r^{*3}}+\frac{\partial^4\xi}{\partial r^{*4}}-\frac{2}{r^*}\frac{\partial^3\xi}{\partial r^*\partial z^{*2}}+2\frac{\partial^4\xi}{\partial r^{*2}\partial z^{*2}}+\frac{\partial^4\xi}{\partial z^{*4}}$
3	$\frac{\partial\psi^*}{\partial\eta}$	0
4	$\frac{\partial^2\psi^*}{\partial\xi^2}$	$\frac{3}{r^{*2}}\left(\frac{\partial\xi}{\partial r^*}\right)^2-\frac{6}{r^*}\frac{\partial\xi}{\partial r^*}\frac{\partial^2\xi}{\partial r^{*2}}+4\frac{\partial\xi}{\partial r^*}\frac{\partial^3\xi}{\partial r^{*3}}+3\left(\frac{\partial^2\xi}{\partial r^{*2}}\right)^2-\frac{4}{r^*}\frac{\partial^2\xi}{\partial r^*\partial z^*}\frac{\partial\xi}{\partial z^*}-\frac{2}{r^*}\frac{\partial^2\xi}{\partial z^{*2}}\frac{\partial\xi}{\partial r^*}+4\left(\frac{\partial^2\xi}{\partial r^*\partial z^*}\right)^2+4\frac{\partial\xi}{\partial z^*}\frac{\partial^3\xi}{\partial r^{*2}\partial z^*}+4\frac{\partial^3\xi}{\partial r^*\partial z^{*2}}\frac{\partial\xi}{\partial r^*}+2\frac{\partial^2\xi}{\partial z^{*2}}\frac{\partial^2\xi}{\partial r^{*2}}+4\frac{\partial^3\xi}{\partial z^{*3}}\frac{\partial\xi}{\partial z^*}+3\left(\frac{\partial^2\xi}{\partial z^{*2}}\right)^2$
5	$\frac{\partial^2\psi^*}{\partial\xi\partial\eta}$	$-\frac{4}{r^*}\frac{\partial^2\xi}{\partial r^*\partial z^*}+4\frac{\partial^3\xi}{\partial r^{*2}\partial z^*}+4\frac{\partial^3\xi}{\partial z^{*3}}$
6	$\frac{\partial^2\psi^*}{\partial\eta^2}$	0
7	$\frac{\partial^3\psi^*}{\partial\xi^3}$	$-\frac{2}{r^*}\left(\frac{\partial\xi}{\partial r^*}\right)^3+6\frac{\partial^2\xi}{\partial r^{*2}}\left(\frac{\partial\xi}{\partial r^*}\right)^2-\frac{2}{r^*}\frac{\partial\xi}{\partial r^*}\left(\frac{\partial\xi}{\partial z^*}\right)^2+2\frac{\partial^2\xi}{\partial r^{*2}}\left(\frac{\partial\xi}{\partial z^*}\right)^2+8\frac{\partial\xi}{\partial r^*}\frac{\partial\xi}{\partial z^*}\frac{\partial^2\xi}{\partial r^*\partial z^*}+2\left(\frac{\partial\xi}{\partial r^*}\right)^2\frac{\partial^2\xi}{\partial z^{*2}}+6\frac{\partial^2\xi}{\partial z^{*2}}\left(\frac{\partial\xi}{\partial z^*}\right)^2$
8	$\frac{\partial^3\psi^*}{\partial\xi^2\partial\eta}$	$-\frac{4}{r^*}\frac{\partial\xi}{\partial r^*}\frac{\partial\xi}{\partial z^*}+4\frac{\partial^2\xi}{\partial r^{*2}}\frac{\partial\xi}{\partial z^*}+8\frac{\partial\xi}{\partial r^*}\frac{\partial^2\xi}{\partial r^*\partial z^*}+12\frac{\partial^2\xi}{\partial z^{*2}}\frac{\partial\xi}{\partial z^*}$
9	$\frac{\partial^3\psi^*}{\partial\xi\partial\eta^2}$	$-\frac{2}{r^*}\frac{\partial\xi}{\partial r^*}+2\frac{\partial^2\xi}{\partial r^{*2}}+6\frac{\partial^2\xi}{\partial z^{*2}}$
10	$\frac{\partial^3\psi^*}{\partial\eta^3}$	0
11	$\frac{\partial^4\psi^*}{\partial\xi^4}$	$\left(\frac{\partial\xi}{\partial r^*}\right)^4+2\left(\frac{\partial\xi}{\partial r^*}\right)^2\left(\frac{\partial\xi}{\partial z^*}\right)^2+\left(\frac{\partial\xi}{\partial z^*}\right)^4$
12	$\frac{\partial^4\psi^*}{\partial\xi^3\partial\eta}$	$4\left(\frac{\partial\xi}{\partial r^*}\right)^2\left(\frac{\partial\xi}{\partial z^*}\right)+4\left(\frac{\partial\xi}{\partial z^*}\right)^3$
13	$\frac{\partial^4\psi^*}{\partial\xi^2\partial\eta^2}$	$2\left(\frac{\partial\xi}{\partial r^*}\right)^2+6\left(\frac{\partial\xi}{\partial z^*}\right)^2$
14	$\frac{\partial^4\psi^*}{\partial\xi\partial\eta^3}$	$4\left(\frac{\partial\xi}{\partial z^*}\right)$
15	$\frac{\partial^4\psi^*}{\partial\eta^4}$	1

APPENDIX B: JACOBI POLYNOMIALS USED IN THE COLLOCATION SOLUTION

The Jacobi polynomials can be expressed as (Villadsen, 1970)

$$P_n^{(\alpha,\beta)}(x) = \sum_{i=0}^{n} (-1)^{n-1}\,\gamma_i x^i$$

with the coefficients γ_i given by the

$$\gamma_o = 1$$

$$\gamma_{i+1} = \frac{n-i}{i+1}\,\frac{n+\alpha+\beta+i+1}{\beta+i+1}\,\gamma_i$$

For the case of $n = 4$, $\alpha = 3$, and $\beta = 0$, these formulas yield the following expression:

$$P_4^{(3,0)}(x) = 1 - 32x + 216x^2 - 480x^3 + 330x^4$$

whose zeroes are 0.042153, 0.209717, 0.464154, and 0.738522.

Manuscript received March 23, 1977; revision received September 7, and accepted September 14, 1977.